Trimeric Inorganic Pyrophosphatase of *Escherichia coli* Obtained by Directed Mutagenesis†

Irina S. Velichko,‡ Katja Mikalahti,§ Vladimir N. Kasho,|| Valeriy Yu. Dudarenkov,‡ Teppo Hyytiä,⊥ Adrian Goldman,§,▽ Barry S. Cooperman,⊥ Reijo Lahti,*,§ and Alexander A. Baykov*,‡

A. N. Belozersky Institute of Physico-Chemical Biology and School of Chemistry, Moscow State University, Moscow 119899, Russia, Department of Biochemistry, University of Turku, FIN-20500 Turku, Finland, Center for Ulcer Research and Education, Department of Medicine, University of California, Los Angeles, California 90073, Department of Chemistry, University of Pennsylvania, Pennsylvania 19104-6323, and Centre for Biotechnology, University of Turku and Åbo Akademi University, FIN-20521 Turku, Finland

Received June 20, 1997⊗

ABSTRACT: *Escherichia coli* inorganic pyrophosphatase is a tight hexamer of identical subunits. Replacement of both His136 and His140 by Gln in the subunit interface results in an enzyme which is trimeric up to 26 mg/mL enzyme concentration in the presence of Mg^{2+}, allowing direct measurements of Mg^{2+} binding to trimer by equilibrium dialysis. The results of such measurements, together with the results of activity measurements as a function of [Mg^{2+}] and pH, indicate that Mg^{2+} binds more weakly to one of the three sites per monomer than it does to the equivalent site in the hexamer, suggesting this site to be located in the trimer:trimer interface. The otherwise unobtainable hexameric variant enzyme readily forms in the presence of magnesium phosphate, the product of the pyrophosphatase reaction, but rapidly dissociates on dilution into medium lacking magnesium phosphate or pyrophosphate. The k_{cat} values are similar for the variant trimer and hexamer, but K_m values are 3 orders of magnitude lower for the hexamer. Thus, while stabilizing hexamer, the two His residues, *per se*, are not absolutely required for active-site structure rearrangement upon hexamer formation. The reciprocal effect of hexamerization and product binding to the active site is explained by destabilization of α-helix A, contributing both to the active site and the subunit interface.

Inorganic pyrophosphatase (EC 3.6.1.1; PPase[1]) is a ubiquitous enzyme, essential for cell growth (Chen et al., 1990; Lundin et al., 1991; Sonnewald, 1992). Soluble PPase hydrolyses PP_i to P_i with release of energy as heat and provides in this way a thermodynamic pull for many biosynthetic reactions, such as protein, RNA, and DNA syntheses (Kornberg, 1962). In contrast, membrane-bound PPase utilizes the energy released for transmembrane H^+ transport (Baltscheffsky & Baltscheffsky, 1992; Rea & Poole, 1993).

The active site structure and catalytic mechanism of soluble PPase are highly conserved evolutionarily (Cooperman et al., 1992; Kankare et al., 1994). Catalysis proceeds without formation of a phosphorylated enzyme (Gonzalez et al., 1984) and exhibits an absolute requirement for divalent metal ions, with Mg^{2+} conferring the highest activity (Kunitz, 1952). Recent crystallographic studies of a complex between yeast PPase, phosphate, and Mn^{2+} have identified four divalent metal ion binding subsites (M1−M4) and two phosphate binding subsites (P1 and P2) within the active site (Heikinheimo et al., 1996; Harutyunyan et al., 1996a).

All soluble PPases are homooligomers, dimers in eukaryotes and hexamers or tetramers in prokaryotes. The active site is present in each monomeric unit. The structure of hexameric *E. coli* PPase is best described as a dimer of two trimers (Kankare et al., 1994; Oganessyan et al., 1994), with His136, His140, and Asp143 being the key residues in the trimer:trimer interface (Kankare et al., 1996b; Harutyunyan et al., 1996b). The interaction between trimers is quite strong and is only broken in acidic medium (Borshchik et al., 1986). A single replacement of any of the two His residues with Gln results in PPase variants existing as a mixture of hexamers and trimers (Baykov et al., 1995). The dyad interface between the trimers has a water-filled cavity, which can accommodate Mg^{2+} (Kankare et al., 1996a; Harutyunyan et al., 1997).

Here we show that substitution of both His residues in the subunit interface of *E. coli* PPase results in a trimeric enzyme with very little tendency to aggregate. We also

† This work was supported by grants from NIH (TW00407 and DK13212), the Russian Foundation for Basic Research (97-04-48487), the Russian State Project Bioengineering, section Enzyme Engineering (1−42), and the Finnish Academy of Sciences (Grants 1444, 3875, 35736, and 4310).

* Authors to whom to address correspondence (R.L.: FAX, 358-2-333-6860; telephone, 358-2-333-6845; email, reila@utu.fi. A.A.B.: FAX, 095-939-3181; telephone, 095-939-5541; email, abaykov@protchem.genebee.msu.su).

‡ Moscow State University.

§ University of Turku.

|| University of California.

⊥ University of Pennsylvania.

▽ Centre for Biotechnology.

⊗ Abstract published in *Advance ACS Abstracts,* November 15, 1997.

[1] Abbreviations: E-PPase, *Escherichia coli* inorganic pyrophosphatase; MgP_i, magnesium phosphate; Mg_2PP_i, dimagnesium pyrophosphate; PPase, inorganic pyrophosphatase; WT, wild-type.

S0006-2960(97)01482-7 CCC: $15.00
Published on Web 01/13/1998

demonstrate a dramatic reciprocal effect of active site ligands on the trimer:trimer interaction and propose a role for the intersubunit divalent metal ion in structure maintenance.

EXPERIMENTAL PROCEDURES

Enzymes. Wild-type and His→Gln mutant PPases were expressed and purified using the overproducing *E. coli* strains HB101 (Lahti et al., 1990) and MC1061/*YPPAI*(Δ*ppa*) (Salminen et al., 1995), respectively. The enzyme concentration was estimated on the basis of a subunit molecular mass of 20 kDa (Josse, 1966) and an $A^{1\%}_{280}$ of 11.8 (Wong et al., 1970).

Methods. Enzyme-bound PP_i was assayed by a modified coupled-enzyme procedure (Nyrén & Lundin, 1985; Baykov et al., 1990). Equilibrated reaction mixtures (50 μL) containing enzyme, P_i, $MgCl_2$, buffer, and EGTA were quenched with 10 μL of 5 M trifluoroacetic acid, kept for 3−5 min at room temperature, and centrifuged for 1 min at 5000*g*. A 5-μL aliquot of the supernatant was added to 0.3 μL of the ATP assay cocktail, and the resulting luminescence was recorded with an LKB model 1250 luminometer. After the luminescence stabilized, 5 μL of 10 μM PP_i solution was added to calibrate the assay. The PP_i assay cocktail was prepared by mixing 6 mL of 0.2 M Tris/HCl buffer (pH 8.0) containing 1 mM dithiothreitol, 0.8 mg/mL bovine serum albumin, 30 μM EGTA, 40 μL of 67 U/mL ATP-sulfurylase solution (Sigma lyophilized preparation reconstituted with water), 200 μL of luciferin/luciferase solution (Sigma ATP assay mix, catalog No. FL-ASC, reconstituted with 5 mL of water) and 60 μL of 1 mM adenosine 5′-phosphosulfate (Sigma).

Details of other kinetic, binding, and sedimentation measurements are described by Baykov et al. (1995, 1996a). The following buffers were used for measurement of steady-state rates of PP_i hydrolysis, except as noted: 83 mM TES/KOH, 17 mM KCl (pH 7.2); 70 mM TAPS/KOH, 30 mM KCl, (pH 8.0); 90 mM TAPS/KOH (pH 8.5); 200 mM CAPS/KOH (pH 9.5 and 10.3). The media used in measurements of enzyme-bound PP_i formation, net PP_i synthesis, and P_i-H_2O oxygen exchange were buffered with Tris/HCl, the concentration of which was adjusted to maintain ionic strength at 0.2 M. The buffers contained EGTA: 50 μM (pH 7.2, 8) or 5 μM (pH 8.5, 9.5). All experiments were performed at 25 °C, except as noted.

Calculations and Data Analysis. The apparent catalytic constant k_h, as well as the apparent Michaelis constant $K_{m,h}$ for PPase catalysis of Mg_2PP_i hydrolysis, was determined as functions of $[Mg^{2+}]$ and pH. Fitting $k_h/K_{m,h}$ to eq 1,

$$\frac{k_h}{K_{m,h}} = \frac{k_1^{(1)}K_{m2}/[Mg^{2+}] + k_1^{(2)} + k_1^{(3)}[Mg^{2+}]/K_{m3}}{1 + K_{m1}K_{m2}/[Mg^{2+}]^2 + K_{m2}/[Mg^{2+}] + [Mg^{2+}]/K_{m3}} \quad (1)$$

derived from Scheme 1 (Baykov et al., 1996a), allowed evaluation of $k_1^{(1)}$, $k_1^{(2)}$, and $k_1^{(3)}$, the second-order rate constants for substrate binding to ME, M_2E, and M_3E, respectively, as well as the dissociation constants K_{m2} and K_{m3} for the corresponding equilibria in Scheme 1. Values of K_{m1} were quite low compared to the metal concentrations

Scheme 1: Equilibria and Binding Steps Defining Formation of Enzyme−Substrate Complex[a]

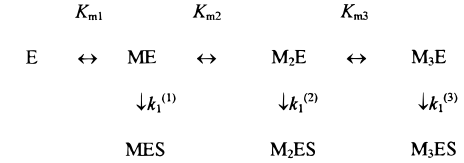

[a] E = enzyme, M = Mg^{2+}, S = Mg_2PP_i.

Scheme 2: Equilibria Linking Species within Enzyme−Substrate Complex

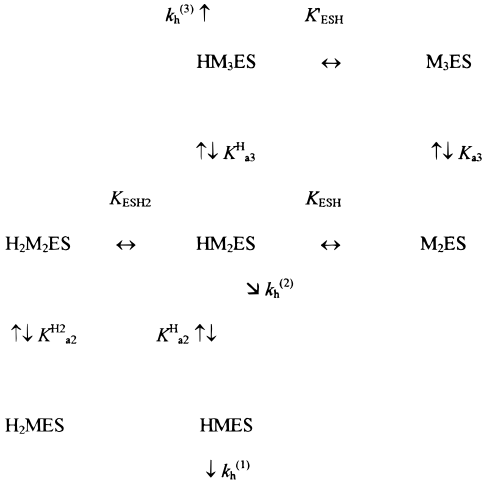

Scheme 3: Hexamer:Trimer Equilibrium

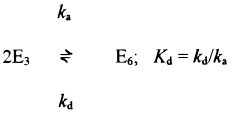

used and were neglected in this analysis. Fitting k_h to eq 2,

$$k_h = \{k_h^{(3)} + k_h^{(2)}K^H_{a3}/[Mg^{2+}]\}/\{1 + K^H_{a3}/[Mg^{2+}] + [H^+]/K_{ESH2}(1 + K^{H2}_{a3}/[Mg^{2+}]) + K_{ESH}/(1 + K_{a3}/[Mg^{2+}])[H^+]\} \quad (2)$$

derived from Scheme 2 (Baykov et al., 1996a), allowed evaluation of $k_h^{(1)}$, $k_h^{(2)}$ and $k_h^{(3)}$, the catalytic constants for HMES, HM_2ES and HM_3ES, respectively, as well as the dissociation constants K_{ESH2}, K'_{ESH}, K_{ESH}, K^{H2}_{a2}, K^H_{a2}, K^H_{a3} and K_{a3} for the corresponding equilibria in Scheme 2.

Equations 3 and 4 describe the equilibrium activity A of a dissociating enzyme system containing hexamers E_6 and trimers E_3 (Scheme 3) as a function of total enzyme concentration $[E]_t$. A_H and A_T are specific activities of hexamer and trimer, respectively, α_H is the fraction of enzyme in the hexameric form at time t, expressed in monomers, and k_a and k_d are the rate constants for hexamer formation and breakdown. Equations 3 and 4 were fitted to data with the program SCIENTIST (MicroMath).

$$A = A_T + (A_H - A_T)\alpha_H \quad (3)$$

$$\frac{d\alpha_H}{dt} = k_a[E]_t(1 - \alpha_H)^2 - k_d\alpha_H = 0 \quad (4)$$

Time-courses of PP_i hydrolysis and synthesis by hexameric (H136,140Q)-PPase undergoing dissociation into less active

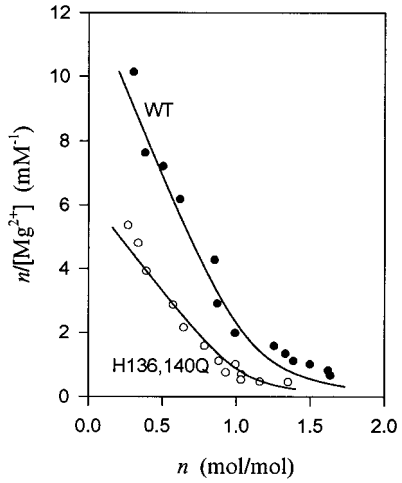

FIGURE 1: Scatchard plot for Mg^{2+} binding to WT-PPase (●) and (H136,140Q)-PPase (○) as measured by equilibrium dialysis (Käpylä et al., 1995). The lines are drawn to eq 4 in Käpylä et al. (1995), using parameter values found in Table 1; *n* measures the number of Mg^{2+} ions bound per monomer. Experimental conditions: 0.1 M Tris/HCl, pH 7.2; [PPase], 0.7−0.8 mM; [Mg^{2+}], 0.03−3 mM.

trimers during catalysis were fit to eq 5, where *t* is time, and v_0 and v_∞ are hydrolysis rates at zero and infinite time, respectively.

$$[\text{product}] = v_\infty t + \frac{v_0 - v_\infty}{k_d}(1 - e^{-k_d t}) \qquad (5)$$

RESULTS

(H136,140Q)-PPase is Trimeric. Three sets of data show that the double variant is trimeric under a wide range of conditions. First, the value of $s_{20,w}$ measured at 26 mg/mL enzyme concentration (pH 7.2, 20 °C, 1 mM $MgCl_2$) was only 3.1 ± 0.1 S (but see below for measurements in the presence of MgP_i). At 0.25 mg/mL enzyme, $s_{20,w}$ was 3.86 ± 0.09 S; the difference can be accounted for by the effect of protein concentration on solution viscosity (Schachman, 1959). For hexameric WT-E-PPase, measured values of $s_{20,w}$ are in the range 6.0−6.2 (Josse, 1966; Baykov et al., 1995). Second, SDS−PAGE of the variant enzyme cross-linked with glutaraldehyde at pH 8.5 yielded polypeptide patterns quite similar to those reported previously for trimeric H136Q- and H140Q-PPases (Baykov et al., 1995), *i.e.*, revealed no hexamer. Third, the specific activity of enzyme in PP_i hydrolysis measured at 20 μM substrate concentration was only 2.5 s^{-1}, characteristic of trimers (see below).

Mg^{2+} Binding to Trimeric (H136,140Q)-PPase. As measured by equilibrium dialysis in combination with atomic absorption spectroscopy (Figure 1), Mg^{2+} binding to one of the two sites seen at pH 7.2 (K_{m2} in Scheme 1) is markedly weakened in trimer (Table 1). These data also indicate a strong buffer effect on the binding parameters: values of both K_{m1} and K_{m2} in WT-PPase hexamer and of K_{m1} in (H136,140Q)-PPase trimer are markedly increased in the presence of Tris/HCl versus TES/KOH buffer (Table 1). Previously we showed that Tris modulates the binding properties of the membrane PPase of *Rhodospirillum rubrum* (Baykov et al., 1996b). As our most recent studies indicate, the Tris is a competitive inhibitor of E-PPase with respect to PP_i (Baykov, A. A., Hyytiä, T., Velichko, I, S., Turkina, M. V., Goldman, A., Lahti, R., & Cooperman, B. S., manuscript in preparation).

Kinetics of PP_i Hydrolysis by Trimeric (H136,140Q)-PPase. Earlier kinetic measurements of H136Q-PPase and H140Q-PPase were performed at a single pH or in a narrow pH range, leaving the possibility that the observed effects of hexamer dissociation resulted from changes in the pK_as of the groups governing the respective pH profiles rather than from changes in the pH-independent values for respective parameters (Baykov et al., 1995). The results of the kinetic measurements of (H136,140Q)-PPase, carried out under wide ranges of pH and Mg^{2+} concentration (Figure 2), rule out this possibility. The model satisfactorily describing the data (Schemes 1 and 2) is similar to that derived previously for WT-PPase (Baykov et al., 1996a) and contains only species whose omission made the fit of eqs 1 and 2 significantly worse. Parameter values derived with eq 1 from the dependencies of $k_h/K_{m,h}$ on [Mg^{2+}] at pH 8.0−10.3 (Table 2) indicate that (a) the values of $k_1^{(1)} - k_1^{(3)}$ are lower for the trimeric variant PPase by 3−4 orders of magnitude compared to hexameric WT-PPase over the whole pH range (Baykov et al., 1996a); (b) substrate is bound more rapidly to EM_2 than to EM_1 and EM_3 ($k_1^{(2)} > k_1^{(3)} > k_1^{(1)}$); and (c) values of K_{m2} for trimeric (H136,140Q)-PPase are significantly higher than for hexameric WT-PPase (Baykov et al., 1996a), in accordance with the data obtained by equilibrium dialysis.

Values of k_h for (H136,140Q)-PPase (Figure 2A) were fitted to eq 2 as a function of [Mg^{2+}] and pH simultaneously, yielding the pK_as and the binding constants shown in Table 3. Because of very weak substrate binding, accurate values of k_h for (H136,140Q)-PPase could not be obtained at pH 7.2. The following trends are evident: (a) neither pH-independent $k_h^{(2)}$ or $k_h^{(3)}$ is decreased markedly in the trimeric PPase; (b) binding of the fourth metal ion to the enzyme−substrate complex (K^{H2}_{a2} and K^{H}_{a2}) is weakened while binding of the fifth metal ion (K^{H}_{a3} and K_{a3}) is strengthened; and (c) the pK_as for the essential acidic and basic groups are increased for catalysis with either four or five Mg^{2+} in the enzyme-substrate complex.

Several lines of evidence rule out the possibility that the activities measured result from hexamer formation during the assay. First, as will be shown below, the hexameric form is unstable under the assay conditions at pH 7.2 and 8.0, and increasing the pH accelerates its dissociation. Second, product formation curves were linear in all cases, indicating no interconversion between trimer and hexamer during measurement. Finally, the rate *versus* substrate concentrations profiles indicated no enzyme heterogeneity, as would have occurred for a mixture of hexamer and trimer with different $K_{m,h}$ values.

Magnesium Phosphate Makes (H136,140Q)-PPase Hexameric. Dramatic stimulation of hexamer formation in the double variant was observed in the presence of MgP_i. The enzyme preincubated with 20 mM MgP_i at pH 7.2 exhibited an initial burst of activity in PP_i hydrolysis and PP_i synthesis (Figure 3, upper curves). No activity burst was detectable when PP_i hydrolysis was initiated by PP_i or when MgP_i was omitted from the preincubation mixture. Similar observations were made at pH 8.0. By contrast, the progress curves in both types of assay were strictly linear with hexameric WT-PPase, which does not dissociate under these conditions.

Table 1: Dissociation Constants for Mg^{2+} Binding to PPase Determined by Equilibrium Dialysis[a]

	hexameric WT-PPase		trimeric (H136,140Q)-PPase	
buffer	K_{m1}	K_{m2}	K_{m1}	K_{m2}
0.1 M Tris/HCl	0.083 ± 0.004[b]	1.67 ± 0.17[b]	0.16 ± 0.02	8 ± 2
0.083 M TES/KOH + 17 mM KCl	0.016 ± 0.002	0.52 ± 0.05	0.008 ± 0.004	5.0 ± 2.5

[a] In millimole per liter. Experimental conditions: pH 7.2; [PPase], 0.7−0.8 mM;, [Mg^{2+}], 0.03−3 mM. [b] From Käpylä et al. (1995).

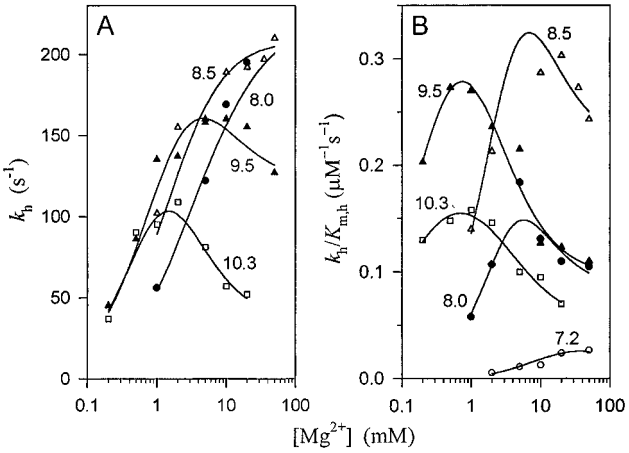

FIGURE 2: Mg^{2+} concentration dependencies of k_h (A) and $k_h/K_{m,h}$ (B) for trimeric (H136,140Q)-PPase at fixed pH values in zwitterionic buffers. The lines are drawn to eqs 1 and 2, using parameter values found in Tables 1 and 2. Values of pH are shown on the curves.

Table 2: Rate and Equilibrium Constants for Trimeric (H136,140Q)-PPase (Scheme 1)

pH	$k_1^{(1)}$ ($\mu M^{-1} s^{-1}$)	$k_1^{(2)}$ ($\mu M^{-1} s^{-1}$)	$k_1^{(3)}$ ($\mu M^{-1} s^{-1}$)	K_{m2} (mM)	K_{m3} (mM)
8.0	<0.02	0.49 ± 0.17	0.09 ± 0.02	7 ± 3	2.2 ± 1.2
8.5	<0.02	0.64 ± 0.36	0.20 ± 0.07	4 ± 2	7 ± 4
9.5	<0.02	0.45 ± 0.15	0.10 ± 0.01	0.23 ± 0.13	1.6 ± 0.8
10.3	<0.02	0.20 ± 0.04	0.05 ± 0.01	0.11 ± 0.06	3.1 ± 1.1

Table 3: Rate and Equilibrium Constants for Hexameric WT-PPase and Trimeric (H136,140Q)-PPase (Scheme 2)

parameter	WT-PPase[a]	H136,140Q-PPase
K^{H}_{a3} (mM)	51 ± 28	11 ± 4
K_{a3} (mM)	3.2 ± 0.8	<2
K^{H2}_{a2} (mM)	0.09 ± 0.05	3.8 ± 2.1
K^{H}_{a2} (mM)	0.05 ± 0.02	0.85 ± 0.09
$k_h^{(1)}$ (s^{-1})	≤120	<40
$k_h^{(2)} = k_h^{(3)}$ (s^{-1})	330 ± 20	227 ± 12
pK'_{ESH}	8.7 ± 0.5	9.56 ± 0.10
pK_{ESH2}	7.31 ± 0.06	7.74 ± 0.19
pK_{ESH}	9.89 ± 0.07	>11

[a] Measured in zwitterionic buffers (Baykov, A.A., Hyytiä, T., Velichko, I. S., Goldman, A., Lahti R., and Cooperman, B. S., manuscript in preparation).

These data suggest that the hexamer that formed in appreciable amounts in the presence of MgP_i in the stock enzyme solution undergoes slow dissociation into trimers on being diluted in assay medium containing Mg_2PP_i or MgP_i or undergoes fast dissociation on being diluted to the media without the substrates. This explanation is supported by two further observations. First, the sedimentation profile of (H136,140Q)-PPase in the presence of 20 mM MgP_i (pH 7.2, 25 °C, 50 mM Mg^{2+}, 18 μM enzyme) indicated the

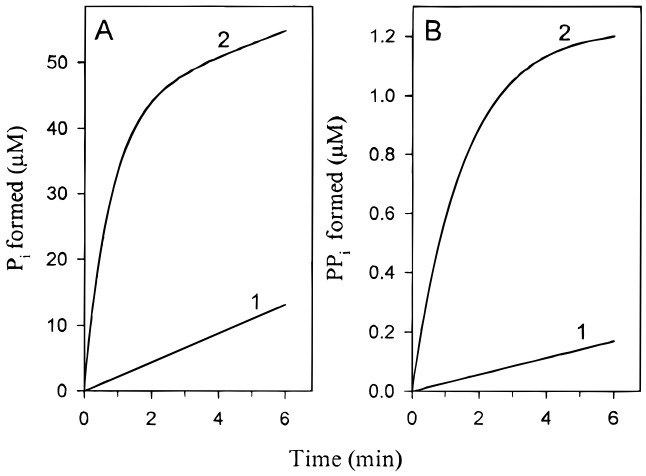

FIGURE 3: Stabilization of hexameric (H136,140Q)-PPase by MgP_i. (A) Time-courses of PP_i hydrolysis by the enzyme preequilibrated at 184 μM concentration in the absence (1) and in the presence (2) of 20 mM MgP_i. In both cases, the preincubation mixture contained 0.06 M Tris/HCl (pH 7.2), 50 mM Mg^{2+}, and 15 μM EGTA. After preincubation for 5 min at 25 °C, an aliquot of enzyme solution was added to the assay medium containing 0.1 mM Mg_2PP_i, 20 mM Mg^{2+}, 0.15 M Tris/HCl (pH 7.2), and 40 μM EGTA, and P_i liberation was continuously recorded. (B) Time-courses of PP_i synthesis by the enzyme preequilibrated at 15 μM concentration as above. The assay medium contained 0.019 μM enzyme, 20 mM MgP_i, 50 mM Mg^{2+}, 0.7 U/mL ATP-sulfurylase, ATP assay kit (Sigma) diluted 1:40, 10 μM adenosine 5-phosphosulfate, 1 mM dithiothreitol, 1 mg/mL bovine serum albumin, 0.15 M Tris/HCl (pH 7.2), and 40 μM EGTA. PP_i formation was followed continuously in an LKB model 1250 luminometer. All curves are experimental; theoretical curves agreed within 3%.

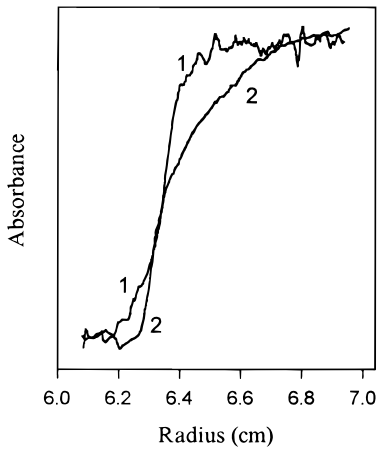

FIGURE 4: Sedimentograms of (H136,140Q)-PPase in the absence (1) and in the presence (2) of 20 mM MgP_i. Experimental conditions: 0.1 M Tris/HCl, pH 7.2; [PPase], 18 μM; [Mg^{2+}], 50 mM; 20 °C; 60 000 rpm; sedimentation time, 46.5 min.

presence of approximately equal amounts of trimers and hexamers, unlike in the absence of MgP_i (Figure 4). Second, the initial specific activity increased as a function of enzyme concentration (Figure 5, upper curve).

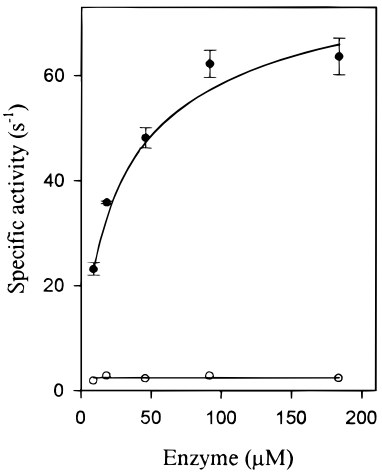

FIGURE 5: Initial specific activity of (H136,140Q)-PPase pre-equilibrated at different enzyme concentrations in the absence (○) and in the presence (●) of 20 mM MgP_i. For conditions, see the legend to Figure 3A. The upper line is drawn to eqs 3 and 4 with $k_d/k_a = 16$ μM, $A_H = 94$ s^{-1}, $A_T = 2$ s^{-1}.

Table 4: Rate and Equilibrium Constants for Scheme 3[a]

pH	substrate present	k_a (μM^{-1} min^{-1})	k_d (min^{-1})	K_d (μM)
7.2			> 70	>5000
7.2	MgP_i (20 mM)	0.05 ± 0.01[b]	0.73 ± 0.04	16 ± 2
7.2	Mg_2PP_i (0.1 mM)		1.1 ± 0.3	
8.0	Mg_2PP_i (0.1 mM)		2.3 ± 0.3	

[a] 25 °C, 50 mM [Mg^{2+}]. [b] Calculated as k_d/K_d.

Values of k_d estimated from the data in Figure 3 with eq 5 and values of K_d estimated from the data in Figure 5 with eqs 3 and 4 are listed in Table 4. One can see that MgP_i and Mg_2PP_i elicited similar changes in k_d, but the value for k_a could be determined only in the presence of MgP_i, because Mg_2PP_i is rapidly hydrolyzed by the enzyme.

Functional Characterization of Hexameric (H136,140Q)-PPase. As described above, fitting eq 5 to the upper curve in Figure 3A provides an estimate of the rate of PP_i hydrolysis by hexameric (H136,140Q)-PPase. Unfortunately, dissociation of hexamers was progressively accelerated when substrate concentration was decreased, limiting our ability to perform such measurements at $[Mg_2PP_i] \leq 50$ μM. Nevertheless, the constancy of the activity (73 ± 3 s^{-1}) in the substrate concentration range of 100−500 μM indicated that the Michaelis constant is less than 20 μM under the conditions used (pH 7.2, 20 mM Mg^{2+}). For hexameric WT-PPase, the Michaelis constant is 2.4 μM under identical conditions (Baykov et al., 1996a).

In addition to its PP_i hydrolysis and PP_i synthesis activities, (H136,140Q)-PPase exhibited appreciable enzyme-bound PP_i formation and rate of P_i/H_2O oxygen exchange (Table 5). On the basis of the large difference in k_1 values between hexamer and trimer and, presumably, PP_i-binding affinity, enzyme-bound PP_i formation and P_i/H_2O oxygen exchange, which occurs during reversible PP_i synthesis (Janson et al., 1979), are mainly due to hexamers, not trimers. This conclusion is further supported by the observation that the value of $v_{ex}/[E]_t$ (exchange rate divided by enzyme concentration) is nearly proportional to enzyme concentration, i.e., changes in parallel with hexamer fraction. Estimates for the rate constant for the reaction $EPP_i \rightarrow E(P_i)_2$ (k_3 in our standard notation; Baykov et al., 1996a) on the hexamer could be obtained with eq 6 (Fabrichniy et al., 1997), where

$$k_3 = \frac{v_{ex}(1 - 0.75P_c)}{f_{epp}[E]_t(1 - P_c)}C \quad (6)$$

P_c is the partition coefficient for oxygen exchange (Hackney & Boyer, 1978), f_{epp} is the fraction of enzyme containing bound PP_i, and C is the correction factor accounting for the difference in hexamer concentration in the assay media used in the measurement of v_{ex} and f_{epp}. The value of C was calculated in each case as the ratio of $v_0 - v_\infty$ values estimated with eq 5 from PP_i hydrolysis curves obtained by starting the reaction with equal aliquots of enzyme taken from the incubation media used in the measurements of EPP_i formation and oxygen exchange. As Table 5 makes clear, the value of k_3 for hexameric (H136,140Q)-PPase is independent of pH and Mg^{2+} concentration and quite close to those for hexameric WT-PPase (Baykov et al., 1996a).

DISCUSSION

Contribution of Different Interactions to Hexamer Stability. The trimer:trimer interface centered around His140 extends through two layers (Figure 6) (Kankare et al., 1994, 1996b; Harutyunyan et al., 1996b). The top layer consists of interactions among His136, His140, and Asp143 at the C-terminus of helix A, the bottom layer of interactions between Ala48 and Phe50 in a little piece of antiparallel β-sheet. The two layers are linked by main-chain and side-chain interactions involving Ser46 and Gln133. The two subunits also interact through a system of hydrogen bonds involving water molecules in the cavity formed by Asn24, Ala25, and Asp26. One of these water molecules can be replaced by an Mg^{2+} ion (Kankare et al., 1996a; Harutyunyan et al., 1997).

All the interactions between trimers can be classified into three groups. The ionic and hydrophobic interactions involving His136, His140, and Asp143 appear to be a key element of the subunit interface. Replacing either of the histidines by glutamine destabilizes hexamer (Baykov et al., 1995), and this work shows that replacing both destroys the interaction completely, making hexamer inaccessible in the absence of magnesium phosphate. The value of K_d in Scheme 3 is <0.001 μM for WT-PPase (Volk et al., 1996) and >5000 μM for (H136,140Q)-PPase (Table 4). The hexameric (H136,140Q)-PPase is thus destabilized by as much as 9 kcal/mol compared to WT-PPase.

A second strong interaction between trimers is mediated by Mg^{2+} binding to enzyme. The value of K_d for H140Q-PPase changes by a factor of 4000 between 1 and 50 mM Mg^{2+} (Baykov et al., 1995), *i.e.*, Mg^{2+} stabilizes hexamer by 5 kcal/mol. Although this effect can in principle result from Mg^{2+} binding to active site, the involvement of the subunit interface site is more likely, as suggested by X-ray crystallographic data showing that the hexamers with metal bound in the subunit interface are more tightly associated than the ones without metal (Kankare et al., 1996a). However, the X-ray data were collected at decimolar Mg^{2+} concentration, raising the possibility that the respective site binds too weakly to be appreciably occupied at millimolar Mg^{2+} concentrations, which are sufficient to stabilize hexamer (Baykov et al., 1995; Volk et al., 1996). In this context,

Table 5: Estimation of k_3 for Hexameric (H136,140Q)-PPase

pH	$[Mg^{2+}]$ (mM)	$[MgP_i]$ (mM)	$[EPP_i]/[E]_o$[a] (mol/mol)	$v_{ex}/[E]_t$[a] (s^{-1})	P_c	k_3[b] (s^{-1})
7.2	50	20	0.094 ± 0.006 (184)	35 ± 2 (6)	0.100 ± 0.010	1350 ± 230
7.2	20	20	0.035 ± 0.003 (184)	16 ± 1 (18)	0.096 ± 0.006	920 ± 350
7.2	20	30	0.094 ± 0.004 (184)	32 ± 4 (18)	0.110 ± 0.004	1250 ± 450
8	20	10	0.010 ± 0.001 (184)	12 ± 1 (12)	0.100 ± 0.003	1340 ± 470

[a] Numbers in parentheses refer to enzyme concentration (μM) used in the corresponding experiment. [b] Estimated with eq 6.

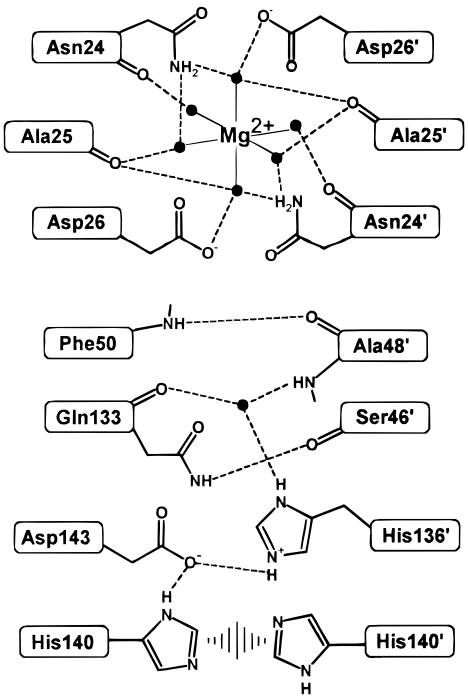

FIGURE 6: A scheme of contacts between dyad-related subunits in *E. coli* PPase (Kankare et al., 1994, 1996b). Unprimed and primed amino acid residue numbers refer to two different subunits. Black circles are water molecules, dashed lines represent hydrogen bonds. Also shown is a hydrophobic contact between His140 and His140′. For clarity, symmetry-related interactions Ala48-Phe50′, Ser46-Gln133′, and His136-Asp143′-His140′ and the interactions of Ala48, Gln133′, and His136 through a water molecule are not shown. The figure is drawn with ChemSketch (ACD Labs).

the equilibrium dialysis data (Table 1), showing greatly decreased affinity of one of the tight metal binding site in trimer, provide further support to this hypothesis.

Based on the estimate of K_d for (H136,140Q)-PPase (Table 2), the remaining interactions contribute in total <3.1 kcal/mol to hexamer stability, assuming no destabilizing interactions of the introduced Gln residues. These weak interactions include three hydrogen bonds formed by the carbonyl oxygen of Ala48 and the side chain of Gln133 with the amide nitrogen of Phe50′ and the carbonyl oxygen of Ser46′, as well as the hydrogen bond between Gln133 and Ser46′, mediated through a water molecule (Figure 6).

Relationship between Quaternary Structure and Catalytic Efficiency. Compared to WT-PPase hexamer, (H136,140Q)-PPase trimer exhibits a greatly decreased rate of substrate binding (k_1; Table 2) and a decreased affinity for the second metal ion in free enzyme (K_{m2}; Table 1) and for the fourth metal ion in enzyme−substrate complex (K^{H}_{a2} and K^{H2}_{a2}). By contrast, the values of the pH-independent catalytic constant are similar for trimer and hexamer (Table 3), consistent with the structures of the corresponding enzyme−substrate complexes being quite similar, though not identical, as indicated by the differences in the pK_as for the acidic and basic groups controlling catalysis (Table 3). The effect of quaternary structure on ligand binding is reciprocal: both MgP_i (and probably Mg_2PP_i) and Mg^{2+} stabilize hexamer.

While the reciprocal effect of Mg^{2+} binding on hexamer formation may result from direct involvement of Mg^{2+} in the trimer−trimer interaction, the effect of MgP_i, which is about 10 Å away from the respective interface, is clearly indirect. A plausible structural explanation can be found in the role of α-helix A (residues 128−140) (Kankare et al., 1996b). It forms an essential part of the active-site cavity, contributes to the hydrophobic core of the molecule, and also makes important contributions to intertrimer contacts. The disruption of the intertrimer contacts upon hexamer dissociation would lead to destabilization of α-helix A in the sense that it would not be positioned accurately along one face of the active site cavity. This would lead to mispositioning of, for instance, Lys142, which binds MgP_i and Mg_2PP_i (Heikinheimo et al., 1996). Conversely, correct positioning of α-helix A can be achieved in two ways: by forming hexamer or by binding substrate/product to the active site. The latter, of course, also stabilizes hexamer over trimer.

Although His136 and His140 are the principal residues stabilizing α-helix A through the trimer−trimer interaction, the results of the present work suggest that the weak bonds involving other residues suffice as well. Both His residues are absent in the trimer:trimer interface of (H136,140Q)-PPase hexamer; nevertheless, its substrate binding affinity, the catalytic constant, and the rate constant for the most important step in catalysis (k_3) are similar to those for WT-PPase hexamer. Thus, while greatly stabilizing quaternary structure, the His interactions, *per se*, are not absolutely required for increasing active site performance upon hexamer formation.

ACKNOWLEDGMENT

The authors thank P. V. Kalmykov for his help in ultracentrifugation, A. Pitt for her help in manuscript preparation, and Dr. V. A. Sklyankina for a helpful discussion.

REFERENCES

Baltscheffsky, M., & Baltscheffsky, H. (1992) in *Molecular Mechanisms in Bioenergetics* (L. Ernster, Ed.), p. 331−348, Elsevier, Amsterdam.

Baykov, A. A., Shestakov, A. S., Kasho, V. N., Vener, A. V., & Ivanov, A. H. (1990) *Eur. J. Biochem. 194*, 879−887.

Baykov, A. A., Dudarenkov, V. Yu., Käpylä, J., Salminen, T., Hyytiä, T., Kasho, V. N., Husgafvel, S., Cooperman, B. S., Goldman, A., & Lahti, R. (1995) *J. Biol. Chem. 270*, 30804−30812.

Baykov, A. A., Hyytiä, T., Volk, S. E., Kasho, V. N., Vener, A. V., Goldman, A., Lahti, R., & Cooperman, B. S. (1996a) *Biochemistry 35*, 4655−4661.

Baykov, A. A., Sergina, N. V., Evtushenko, O. A., & Dubnova, E. B. (1996b) *Eur. J. Biochem. 236*, 121−127.

Borshchik, I. B., Magretova, N. N., Chernyak, V. Ya., Sklyankina, V. A., & Avaeva, S. M. (1986) *Biokhimiya 51*, 1484−1489.
Cooperman, B. S., Baykov, A. A., & Lahti, R. (1992) *Trends Biol. Sci. 17*, 262−266.
Fabrichniy, I. P., Kasho, V. N., Hyytiä, T., Salminen, T., Halonen, P., Dudarenkov, V. Yu., Heikinheimo, P., Chernyak, V. Ya., Goldman, A., Lahti, R., Cooperman, B. S., & Baykov, A. A. (1997) *Biochemistry 36*, 7746−7753.
Gonzalez, M. A., Webb, M. R., Welsh, K. M., & Cooperman, B. S. (1984) *Biochemistry 23*, 797−801.
Hackney, D. D., & Boyer, P. D. (1978) *Proc. Natl. Acad. Sci. U.S.A. 75*, 3133−3137.
Harutyunyan, E. H., Kuranova, I. P., Vainshtein, B. K., Hohne, W. E., Lamzin, V. S., Dauter, Z., Teplyakov, A. V., & Wilson, K. S. (1996a) *Eur. J. Biochem. 239*, 220−228.
Harutyunyan, E. H., Oganessyan, V. Yu., Oganessyan, N. N., Terzyan, S. S., Popov, A. N., Rubinskiy, S. B., Vainshtein, B. K., Nazarova, T. I., Kurilova, S. A., Vorobjeva, N. N., & Avaeva, S. M. (1996b) *Kristallografiya 41*, 84−96.
Haruryunyan, E. H., Oganessyan, V. Yu., Oganessyan, N. N., Avaeva, S. M., Nazarova, T. I., Vorobyeva, N. N., Kurilova, S. A., Huber, R., & Mather, T. (1997) *Biochemistry 36*, 7754−7760.
Heikinheimo, P., Lehtonen, J., Baykov, A.A., Lahti, R., Cooperman, B. S., & Goldman, A. (1996) *Structure 4*, 1491−1508.
Janson, C. A., Degani, C., & Boyer, P. D. (1979) *J. Biol. Chem. 254*, 3743−3749.
Josse, J. (1966) *J. Biol. Chem. 241*, 1938−1947.
Kankare, J., Neal, G. S., Salminen, T., Glumhoff, T., Cooperman, B. S., Lahti, R., & Goldman, A. (1994) *Protein Eng. 7*, 823−830.
Kankare, J., Salminen, T., Lahti, R., Cooperman, B., Baykov, A. A., and Goldman, A. (1996a) *Biochemistry 35*, 4670−4677.
Kankare, J., Salminen, T., Lahti, R., Cooperman, B., Baykov, A. A., & Goldman, A. (1996b) *Acta Crystallogr. D, 52*, 551−563.
Käpylä, J., Hyytiä, T., Lahti, R., Goldman, A., Baykov, A. A., & Cooperman, B. S. (1995) *Biochemistry 34*, 792−800.
Kunitz, M. (1952) *J. Gen. Physiol. 35*, 423−449.
Lahti, R., Pitkäranta, T. Valve, E., Ilta, I., Kukko-Kalske, E., & Heinonen, J. (1988) *J. Bacteriol. 170*, 5901−5907.
Lahti, R., Pohjanoksa, K., Pitkaranta, T., Heikinheimo, P., Salminen, T., Meyer, P., & Heinonen, J. (1990) *Biochemistry 29*, 5761−5766.
Lahti, R., Salminen, T., Latonen, S., Heikinheimo, P., Pohjanoksa, K., Pitkaranta, T., & Heinonen, J. (1991) *Eur. J. Biochem. 198*, 293−297.
Lundin, M., Baltscheffsky, H., & Ronne, H. (1991) *J. Biol. Chem. 266*, 12168−12172.
Nyrén, P., & Lundin, A. (1985) *Anal. Biochem. 151*, 504−509.
Oganessyan, V. Yu., Kurilova, S. A., Vorobjeva, N. N., Nazarova, T. I., Popov, A. N., Lebedev, A. A., Avaeva, S. M., & Harutyunyan, E. H. (1994) *FEBS Lett. 348*, 301−304.
Rea, P. A. & Poole, R. J. (1993) *Annu. Rev. Plant Physiol. Plant Mol. Biol. 44*, 157−180.
Salminen, T., Käpylä, J., Heikinheimo, P., Kankare, J., Goldman, A., Heinonen, J., Baykov, A. A., Cooperman, B. S., & Lahti, R. (1995) *Biochemistry 34*, 782−791.
Schachman, H. K. (1959) *Ultracentrifugation in Biochemistry*, Academic Press, New York.
Sonnewald, U. (1992) *Plant J. 2*, 571−581.
Volk, S. E., Dudarenkov, V. Yu., Käpylä, J., Kasho, V. N., Voloshina, O. A., Salminen, T., Goldman, A., Lahti, R., Baykov, A. A., & Cooperman, B. S. (1966) *Biochemistry 35*, 4662−4669.
Wong, S. C. K., Hall, D. C., & Josse, J. (1970) *J. Biol. Chem. 245*, 4335−5345.

BI9714823